Preprints.org

Article

Not peer-reviewed version

Design and Investigation of Hybrid Microfluidic Micromixer

Muhammad Waqas , Giedrius Janusas , Vytenis Naginevičius , Arvydas Palevicius *

Posted Date: 27 April 2024

doi: 10.20944/preprints202404.1780.v1

Keywords: Micro-mixing; Acoustic streaming; Acoustofluidics; Microfluidics; Mixing index

Preprints.org is a free multidiscipline platform providing preprint service that is dedicated to making early versions of research outputs permanently available and citable. Preprints posted at Preprints.org appear in Web of Science, Crossref, Google Scholar, Scilit, Europe PMC.

Copyright: This is an open access article distributed under the Creative Commons Attribution License which permits unrestricted use, distribution, and reproduction in any medium, provided the original work is properly cited.

Preprints.org (www.preprints.org) | NOT PEER-REVIEWED | Posted: 27 April 2024 doi:10.20944/preprints202404.1780.v1

Disclaimer/Publisher's Note: The statements, opinions, and data contained in all publications are solely those of the individual author(s) and contributor(s) and not of MDPI and/or the editor(s). MDPI and/or the editor(s) disclaim responsibility for any injury to people or property resulting from any ideas, methods, instructions, or products referred to in the content.

Article

Design and Investigation of Hybrid Microfluidic Micromixer

Muhammad Waqas [1], Giedrius Janusas [1], Vytenis Naginevicius [2] and Arvydas Palevicius [1,*]

[1] Faculty of Mechanical Engineering and Design, Kaunas University of Technology; muhammad.waqas@ktu.edu; giedrius.janusas@ktu.lt; arvydas.palevicius@ktu.lt
[2] Faculty of Applied Sciences, Kaunas University of Applied Engineering Sciences, 50155 Kaunas, Lithuania; vytenis.naginevicius@edu.ktk.lt
* Correspondence: arvydas.palevicius@ktu.lt

Abstract: Nowadays, microfluidics has become an anarchist interdisciplinary topic with considerable attention in a wide range of biotechnology applications. In this research work, numerical investigation of microfluidic micro-mixer is carried out using hybrid actuation approach with different micropillar shapes and gaps. For this purpose, COMSOL Multiphysics is used with three different physics such as thermoviscous acoustic to solve acoustic governing equations, laminar physics is used to solve fluid flow governing equations and diluted transport species is used to solve mixing governing equations. The simulations were carried out with flow velocity of 200 μm/s at both inlets with an oscillation frequency of 15kHz. The outcomes were in the form of acoustic characteristics such as acoustic pressure, acoustic velocity, acoustic streaming and mixing index. The results revealed that the inclusion of micropillars enhanced the mixing performance and strength of acoustic field resulting in improvement of mixing performance compared to the case without micropillars. In addition, it was also investigated that blade shape micropillars with 0.150 mm gaps deliver best results compared to the other cases with maximum and minimum values of the mixing index 0.95 and 0.72 respectively. The obtained results can be extremely helpful for design and modifications of hybrid microfluidics micro-mixer.

Keywords: micro-mixing; acoustic streaming; acoustofluidics; microfluidics; mixing index

1. Introduction

Nowadays, microfluidics has become revolutionary interdisciplinary topic with considerable interest in a broad range of bioengineering applications such as mixing, sorting, separation, detection and reaction [1]. Microfluidics devices are the best replica of conventional lab due to its unique abilities such as small sample consumption, and exact control of fluid particles at micro scale [2]. In addition, the microfluidics have unique properties, such as high surface area-to-volume ratios and rapid mass and heat transfer, have paved the way for innovations in a variety of scientific and commercial fields, promising increased efficiency, portability, and cost-effectiveness across a wide range of applications [3]. In microfluidics devices, the manipulation of fluid particles is challengeable through microchannels with dimensions ranging from micrometers to millimeters. High degree of mixing of biofluids and biochemicals is a crucial feature in many microfluidics devices, aiming to get homogeneous mixture between two different heterogeneous components at laminar flow conditions with minimum fabrication complexity [4]. Over the decades, numerous studies have been carried out and several microfluidics micromixers have been proposed. Moreover, extensive literature shows a wide categorization of microfluidics micromixers into two major types such as active and passive micromixers based on external energy supply in order to operate [5].

Active micromixers need external sources such as electric fields, acoustic field, magnetic field and photothermal effect to operate and control the mixing fluids [6]. These source cause disturbance in the flowing fluid pattern leads to enhancement of heterogeneous fluids species transport [7]. Such kind of disturbance enhances the interfacial area between two different heterogeneous fluids. Chandan Kumar et al. [8] developed a numerical model in order to simulation transportation

© 2024 by the author(s). Distributed under a Creative Commons CC BY license.

Preprints.org (www.preprints.org) | NOT PEER-REVIEWED | Posted: 27 April 2024 doi:10.20944/preprints202404.1780.v1

phenomena in microfluidics systems with fluorescent and ferrofluid dye which was induced by the nonuniform magnetic source. Masoud Rahimi et al. [9] demonstrated the impact of ultrasound wave on mixing performance of T- type micromixer. They used piezoelectric transducers to generate vibration. Habib Jalili et al. [10] examined the optimization of effective parameters and their impact on the mixing quality in 2D active type micromixer. Yanwen Gong et al. [11] investigated the concentration field and flow distribution in the microchannel and observed two different circulation flows and four various rotating vortices produced in the expansion micromixer chamber by inducing of AC electric fields. Siyue Xiong et al. [12] proposed a novel type rhombic electroosmotic micromixer by using the principles of both convergence and divergence with microelectrodes in order to enhance mixing performance. They examined the performance of micromixer by changing the rhombic angle and the combination of various rhombic elements. Bappa Mondal et al. [13] investigated the mixing and flow characteristics of heterogeneous charged micromixer numerically for an electroosmotic flow with obstacles both at top and bottom walls. Kasavajhula Naga Vasista et al. [14] examined the electroosmotic mixing attributes for fluid flow by hydrophobic microchannel with interfacial slip subjected to different surface charge. They also developed a theoretical framework to solve the Poisson–Boltzmann equation.

On the other hand, passive micro-mixers do not depend on any external energy source for fluid manipulation and actuation purposes [15]. In passive mixer, the geometrical features of microchannel are utilized in many microfluidics systems because of its larger system stability [16]. Moreover, mass transfer is also dominated in passive microfluidics system by molecular diffusion and convection shortening the diffusion paths [17]. Passive micromixers were used to create nanoparticles in continuous, batch, or semi-batch modes [18]. ZhenghaoWang et al. [19] reported a 3D PDMS microfluidics micromixers based on splitting-stretching and then recombining of fluids streams in order to enhance diffusion which increase the mixing with low Reynolds numbers. Yice Shao et al. [20] examined the impact of microchannel width, applied voltage and waveform on fluid mixing and flow characteristics by means of numerically and experimentally. They used a passive approach to investigate the mixing performance of micromixer. Kevin Ward et al. [21] explored a novel approach in order to improve mixing within the microfluidics devices for various applications. They also used ridges or slanted walls and varied the various geometrical configurations and patterns to evaluate the mixing performance of microfluidics device using numerical simulations. Jae Bem You et al. [22] developed a Y- shaped turbulent microfluidics micromixer which is made of PDMS and glass substrate in order to investigate the mixing performance using experimental and numerical approaches. Xueye Chen et al. [23] used fractal principle with multi-objective genetic algorithm and multi-objective optimization of the cantor fractal baffle microfluidics micromixer in order to investigate the mixing performance at different Reynolds numbers. A. Farahinia et al. studied the optimal design of passive T-mixer which involved the prescribed pattern of barriers and furrows with various geometrical configurations using numerical approach. Min Xiong et al. [24] conducted a topology optimization in order to enhance the mixing performance for microfluidics micro-mixers based om principle of Tesla valve.

Nowadays, acoustic wave-based approach has been extensively applied in order to facilitate microfluidics mixing because of its flexible control, short mixing distance and intensive kinetic of biofluids [25]. Acoustic radiation and acoustic streaming are the two main phenomena that are used in microfluidics. The acoustic radiation force refers to the time averaged force resulting from the time harmonic nature of acoustic waves. On the other hand, the averaged flow produced by the nonlinear interaction of the time harmonic acoustic fields is known as acoustic streaming [26]. In addition, some microstructures or microbubbles were added into the micro channel to improve acoustic streaming and mixing efficiency [27]. As a result, adaptable acoustic-facilitated micromixers have been used in a variety of domains, including materials synthesis, cell manipulation, and enzyme bioassay [28].

Mixing efficiency is an important parameter to measure proper mixing of heterogeneous biofluids and biochemicals [29]. There are several factors such as total flow rate, flow rate ratio and other geometrical features which influence the mixing performance in microfluidics systems. While greater flow rates result in shorter contact area in the microchannels and shorter mixing time [30]. On

Preprints.org (www.preprints.org) | NOT PEER-REVIEWED | Posted: 27 April 2024 doi:10.20944/preprints202404.1780.v1

the other hand, lower flow rate ratio might result in thinner layers which are wrapped by the sheath flow in a flow focus area and thus shorter diffusion in lengths. Moreover, geometrical shapes in microfluidic channels are also influenced on mixing performance [31]. There are two common kinds of mixing geometry in passive microfluidics systems which greatly rely on laminar diffusion mechanism, consequently limiting their mixing effectiveness. Most of the researchers have explored numerous geometries modifications aiming enhancement of interfacial area in order to increase and improve the mixing performance [32]. Generally, two kinds of microchannels (T-Shape & Y-Shape) are widely used for mixing purposes in microfluidics systems. Fengli Liu et al. [33] proposed a novel type micromixers based on flexible artificial cilium which is actuated by magnetic field. They used cilium structure in a circular micro chamber which was then compared with pure diffusion and observed that up to 80% of a 60 micro liter fluid in the chamber was fully mixed after 2 minutes under magnetic flux of 22mT for 20 minutes. A more comprehensive literature review about active and passive actuation approach is listed in Table 1.

Table 1. Summary of various micromixers design.

Year	Goal	Microchannel Type	Microfluidic Type	Microchannel Design	References
2023	Development and characterization of 3D zig-zag microchannel.	3D Zig-Zag microchannel	Passive	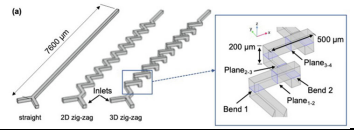	[5]
2023	Investigate impact of geometrical parameters and applied voltage on fluid mixing and fluid flow behavior experimentally and numerically.	Cross channel	Active	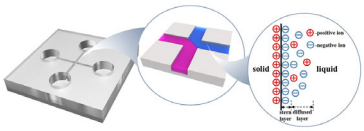	[20]
2023	Introduced acoustic fluid approach to control chemical concentration within picolitre droplet in disposable microfluidic chip.	T-Shape	Hybrid (Active & Passive)	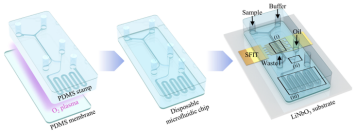	[34]
2023	Investigation of fluid flow mixing in fractal tree.	Fractal Tree	Passive	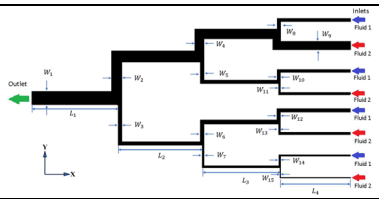	[32]
2023	Topology optimization of micromixers based on tesla principle valve.	Tesla based shape	Passive	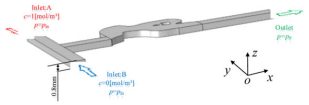	[24]
2022	Development and analysis of microfluidics system with thermal control unit to reduce thermal affect due to acoustic actuation.	Double Y-Shape	Active	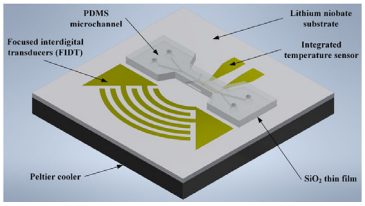	[7]

Preprints.org (www.preprints.org) | NOT PEER-REVIEWED | Posted: 27 April 2024 doi:10.20944/preprints202404.1780.v1

2022	Introduced novel type microfluidic microchannel design for sequential RBC's separation and lysis.	Y-Shape and Zig-Zag Shape	Passive	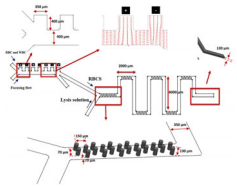	[35]
2022	Investigation of different operational parameters by combining fractal principle with multi objective genetic algorithm and multi objective optimization of cantor fractal baffle micromixers.	Cantor fractal baffle shape micromixers	Passive	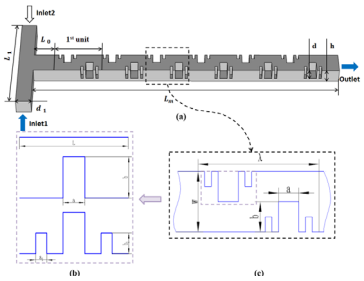	[23]
2019	Design and optimization of active based microchannel incorporated with Micropillars.	Microchannel with Micropillars	Hybrid (Active & Passive)	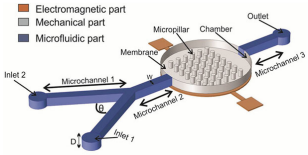	[36]

According to current literature, it has been concluded that the actuation of fluid particles in microfluidics systems especially for mixing applications is necessary to improve the performance of the system. In addition, most of the authors used passive approaches such as different geometrical configurations and parameters to reduce energy consumption and miniaturized microfluidics system. Authors have been worked on different design configurations such as Y-shape, T-shape, zigzag, circular chamber with Micropillars, tesla based microchannels, cross shape channels, Cantor fractal baffle shape micromixers, fractal tree shape with asymmetric microchannels etc. On the other hand, some authors used active actuation approaches such as electromagnetic, acoustic, photothermal to manipulate the fluid particles especially for mixing applications. Moreover, it has also been examined that a very less work conducted on hybrid approach in which combine active and passive approach is used for mixing applications. A hybrid microfluidic approach might offer numerous advantages to generate more versatile and efficient microfluidics system such as increase control and precision of flowing fluid, reduce energy consumption, flexibility, and versatility, enhance mixing performance etc. Thus, there is a great potential exists in using hybrid approach in design, development, and research microfluidics system for controlling and manipulation of fluid particles especially for mixing applications.

The main objective of this research work is to evaluate mixing performance of microfluidics micro-mixer with different micro-pillars shape and different micro-pillars gap numerically using hybrid actuation approach. The nature of acoustic streaming velocity, acoustic velocity and acoustic pressure were also investigated in the presence of micro-pillars with different gaps. Thereafter, based on these characteristics, mixing performance was evaluated because of acoustic streaming and their impact on species transport. The findings from this study also demonstrated how the proposed hybrid microfluidics micro-mixer can enhance the mixing index between two different heterogeneous species. The obtained results in this study can be extremely helpful for design and modifications of microfluidics micro-mixers for high quality mixing of fluids.

2. Materials and Methods

This section describes the research scheme in which three different stages are developed to conduct current research work. In the first stage, a selection of conceptual designs of microfluidics micro-mixer are finalized with suitable geometrical features. The schematic diagrams of four different microfluidics micro-mixer designs are shown in Figure 2. In the second stage, numerical

Preprints.org (www.preprints.org) | NOT PEER-REVIEWED | Posted: 27 April 2024 doi:10.20944/preprints202404.1780.v1

simulations are performed using hybrid actuation approach based on chosen micro-mixer designs. In the third stage, findings from numerical simulations are analyzed and compared with previous studies for validation purposes.

2.1. Micro-Mixer Design and Performance Parameters

Figure 2 describes the four different designs of microfluidics micro-mixers with geometrical features. The presented four geometries are differentiated by different micropillars shapes inside the microchamber. Figure 1(a) is a plane micro-mixing chamber with no micropillars. Figure 1(b) represents a micro-mixing chamber with circular shape micropillars which increase the acoustic streaming leads to higher mixing performance. Similarly, Figure 1(c) represents the third micro-mixer design with hexagonal shape micropillars which help to attain a homogeneous mixing of two different heterogeneous fluids components at laminar flow conditions. Figure 1 (d) represents the fourth micro-mixer design with blade shape micropillars generate more vortices around the micropillars walls. The edges of blade shaped micropillars help to increase mixing performance of two different heterogeneous fluids.

On the other hand, performance of the micro-mixer is measured in terms of mixing index and concentration of two different heterogeneous fluid components at outlet of the micro-mixer. The mixing index is measured based on the statistical approach. It is determined at any cross-section of the microchannel width from the standard deviation of the heterogeneous fluid species concentration using the following relation [19].

$$M = 1 - \sqrt{\frac{\sigma^2}{\sigma^2_{\max}}} \quad (1)$$

$$\sigma = \sqrt{\frac{1}{n}\sum_{i=1}^{n}(c_i - \bar{c})} \quad (2)$$

$$\sigma_{\max} = \sqrt{\bar{c}(1-\bar{c})} \quad (3)$$

Where σ is standard deviation and c_i is the concentration species of two different heterogeneous fluids, $\bar{c}$ is the mean concentration of two different heterogeneous fluids and $\sigma_{\max}$ is the value of maximum standard deviation of the two various heterogeneous fluids species at specified cross section of the micromixer channel.

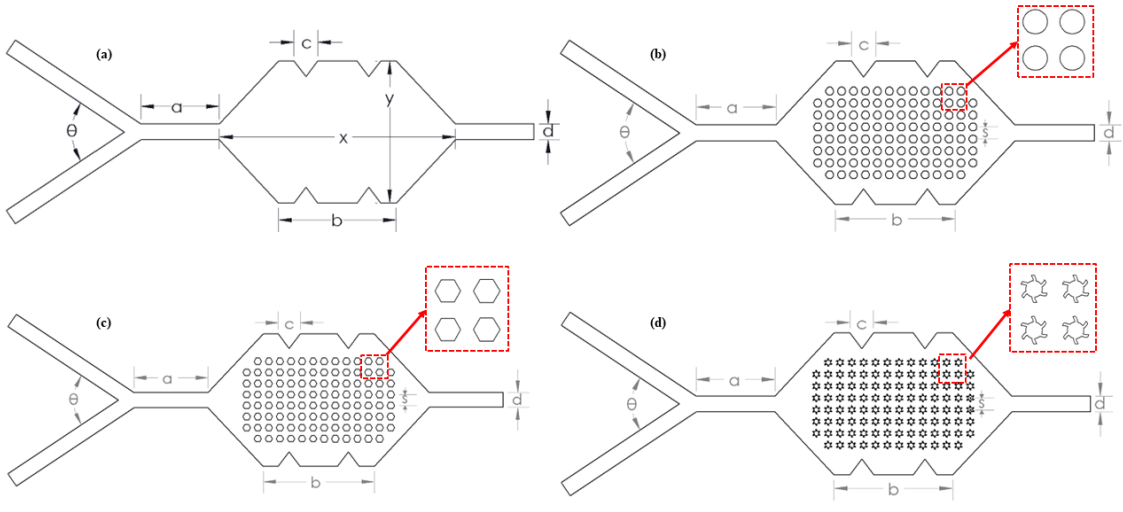

a = 1 mm b = 1.5 mm c = 0.3 mm d = 0.2 mm θ = 67.36° x = 3 mm y = 1.8 mm Dia. Of micropillars= 0.1 mm

S = 0.150mm, 0.175 mm, 0.200 mm, 0.225 mm & 0.250 mm

Figure 1. Four different geometries of micromixers; (a) plane mixing chamber (b) mixing chamber with circular micropillars (c) mixing chamber with hexagonal micropillars (d) mixing chamber with blade type micropillars.

Preprints.org (www.preprints.org) | NOT PEER-REVIEWED | Posted: 27 April 2024 doi:10.20944/preprints202404.1780.v1

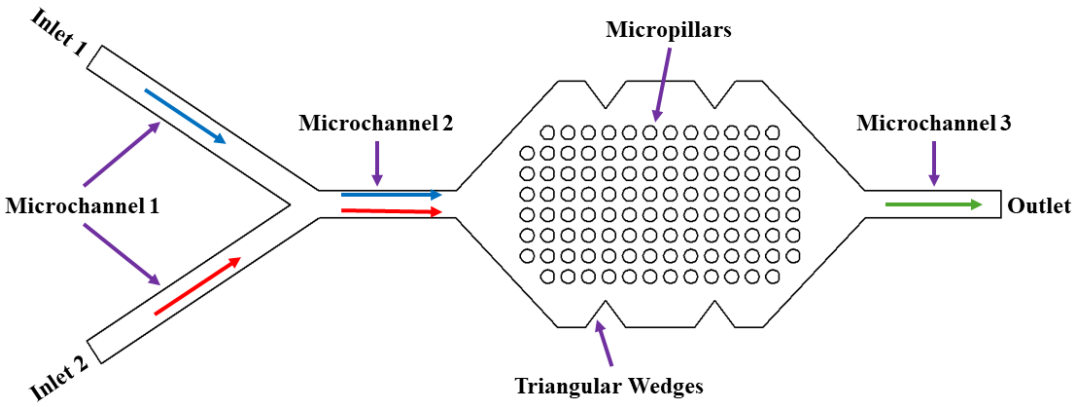

Figure 2. Two-dimensional computational domain for numerical simulations.

2.2. Computational Domain and Meshing

In this research work, numerical simulations of four different micro-mixer designs are carried out to investigate the mixing performance using hybrid actuation approach. The numerical scheme is used to solve the 2D computational domain of micro-mixer which has three microchannels, two inlets, one outlet and one mixing chamber contain micropillars as shown in Figure 2. For numerical simulations, COMSOL Multiphysics is used. In addition, the meshing of micro-mixer models is also done using COMSOL Multiphysics as shown in Figure 3. The observed total number of elements and nodes are 30012 and 17821 respectively. The overall mesh quality lies in an acceptable range.

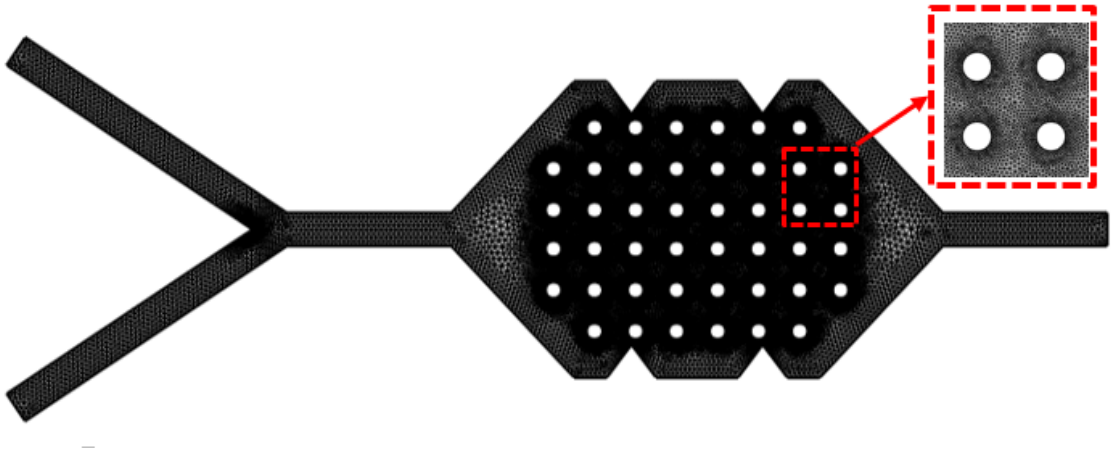

Figure 3. Meshing of micro-mixer for numerical simulations.

2.3. Mathematical Modeling

Mathematical modeling generally describes the behavior of acoustic phenomena and their interaction with flowing fluids in an acoustic mixing inside the microchannels. Acoustic mixing is a technique which uses acoustic waves to generate motion in the flowing fluid. In this section, a detailed description and mathematical relations of governing equations needed for the simulation of acoustic mixing have been discussed. The governing equations related to mass and momentum conservation such as continuity equation and Navier-Stokes equation are described respectively. In addition, three different numerical models such as thermoviscous acoustic model in which governing equations are obtained from linearized Navier-Stokes equations which can be used to solve continuity and momentum in the microchannels, Laminar flow model that solve the flow governing equations and transport diluted species model that is used to determine mixing index. Furthermore, the boundary conditions applied on the micromixer have also been elaborated.

Preprints.org (www.preprints.org) | NOT PEER-REVIEWED | Posted: 27 April 2024 doi:10.20944/preprints202404.1780.v1

2.3.1. Mass and Momentum Conservation

The governing equations related to mass and momentum conservation such as equation of continuity and Navier-Stokes equations for compressible Newtonian fluids are given below [37].

$$\frac{\partial \rho}{\partial t} + \nabla.(\rho v) = 0 \quad (4)$$

$$\rho \frac{\partial v}{\partial t} + \rho(v.\nabla)v = -\nabla p + \mu \nabla^2 v + \beta \mu \nabla(\nabla.v) \quad (5)$$

Where ρ is the fluid density, μ is the dynamic viscosity of the fluid, β represents the viscosity ratio, p and v describe the pressure and velocity of the flowing fluid respectively.

2.3.2. Thermoviscous Acoustic Model

Thermoviscous acoustic model generally describes the behavior of acoustic waves with flowing fluids considering both viscous and thermal effects. This model plays an important role to predict behavior of acoustic waves accurately in a system where viscous and thermal effects are involved. Thermoviscous acoustic model is useful to solve coupled partial differential equations such as Navier-Stokes equation for flowing fluid and coupled with the governing equations which involved heat conduction and acoustic wave equations. The governing equations for thermoviscous acoustic model in frequency domain is given below [38].

$$i\omega\rho_t + \nabla.(\rho_o u_t) = 0 \quad (6)$$

$$i\omega\rho_o u_t = \nabla.\rho_o \quad (7)$$

$$\sigma = -\rho_t 1 + \mu(\nabla u_t + (\nabla u_t)^T) - (\frac{2}{3}\mu - \mu_B)(\nabla.u_t)1 \quad (8)$$

$$\rho_t = \rho_o 1(\beta_T p_t - \alpha_p T_t) \quad (9)$$

$$\rho_t = p + p_b',\ u_t = u + u_b',\ T_t = \frac{\alpha_p T_o}{\rho_o C_p} p + T_b \quad (10)$$

Where ω is natural frequency, μ represents the dynamic viscosity, u_t is wave velocity, T describes the fluid temperature and C_p is specific heat capacity at constant pressure, β_T describes the compressibility of fluid at constant temperature and α_p is the coefficient of thermal expansion.

2.3.3. Laminar Model

Laminar model represents a mathematical approach that is used to describe the behaviour of flowing fluid in a laminar condition. The governing equations related to laminar model is given below [39].

$$\rho(u2.\nabla)u2 = \nabla.[-p21 + K] + F \quad (11)$$

$$\rho\nabla.u2 = 0 \quad (12)$$

Where K describes the thermal effect in the flowing fluid and F is the external volume force exerted in the fluid.

2.3.4. Transport Diluted Species Model

The transport diluted species model is generally used to describe the mixing of two different chemically active species. In this work, the transport diluted species model is used to solve the advection-diffusion equations after considering the consumption rate and production of reactants and products respectively. The governing equations for transport diluted species in frequency domain are given below [40].

$$\nabla.j_i + u.\nabla c_i = R_i \quad (13)$$

$$j_i = -D_i \nabla c_i \quad (14)$$

Preprints.org (www.preprints.org) | NOT PEER-REVIEWED | Posted: 27 April 2024 doi:10.20944/preprints202404.1780.v1

Where c is the concentration of species, D is the diffusion coefficient, R represents the reaction rate for reactant species and j is the mass flux factor that describes the diffusive flux vector.

2.4. Numerical Scheme and Boundary Conditions

In this work, numerical simulations of hybrid microfluidics micro-mixer are carried out as well as governing equations are solved using Finite Element Method (FEM) in COMSOL Multiphysics. A detailed description of numerical methodology is shown in Figure 4. There are three different schemes such as thermoviscous acoustic scheme that is used to solve acoustic related equations, laminar scheme is used to solve fluid flow equations with laminar behavior and transport diluted species scheme that is used to determine the mixing performance of the system. The walls of the microchannel assumed solid wall and stationery with no slip and zero velocity conditions. Thus, the flowing fluid at both inlet is assumed as fully developed and uniform with inlet flow velocity of 200μm/s and oscillation frequency is set to 15 KHz. The pressure boundary condition is set to zero at both inlets and absolute pressure at outlet. Similarly, the concentration of two different species was set to 1 mol/m^3 at one inlet and zero at another inlet. Table 2 listed the material properties of working fluids water and ethanol such as density, dynamic viscosity, specific heat capacity ratio, thermal expansion, and thermal diffusivity etc.

Table 2. Material properties of water and ethanol.

Properties	Water	Ethanol
Viscous dynamic viscosity	890 μPas	1200 μPas
Specific heat capacity	4180 J/kg.K	2570 J/kg.K
Density	997 kg/m^3	789 kg/m^3
Speed of sound	1497 m/s	1144 m/s
Compressibility	4.47x10-10 1/Pa	1.1x10-9 1/Pa
Specific heat capacity ratio	1.012	1.13
Thermal conductivity	0.61 W/m.K	0.614 W/m.K
Thermal expansion coefficient	2.74x10-4 1/K	1.09x10-3 1/K
Thermal diffusivity	1.464x10-7 m^2/s	7x10-8 m^2/s
Bulk dynamic viscosity	2.47 mPas	1.2 mPas

Preprints.org (www.preprints.org) | NOT PEER-REVIEWED | Posted: 27 April 2024 doi:10.20944/preprints202404.1780.v1

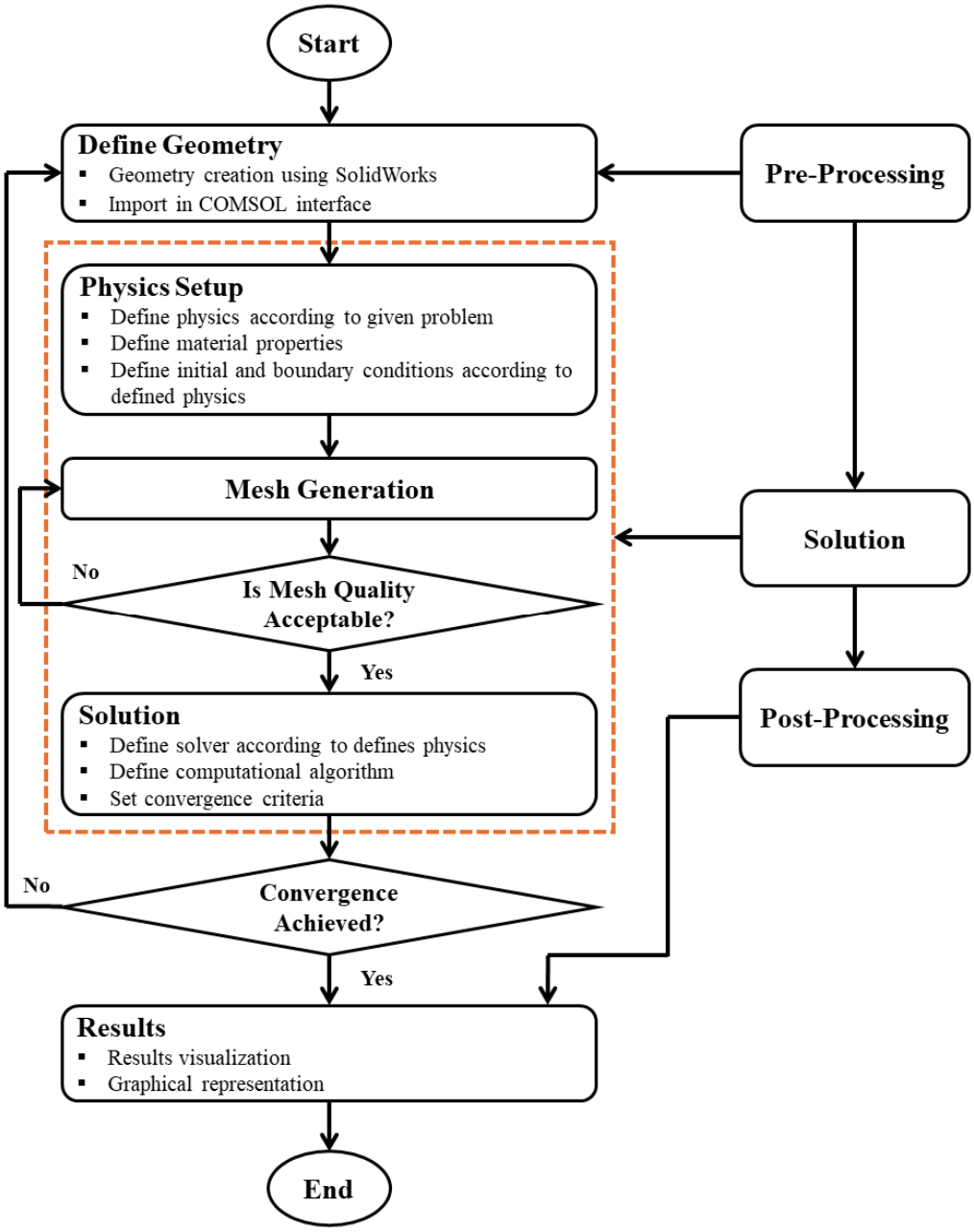

Figure 4. Numerical research methodology flow chart.

3. Mesh Independence Study

Optimal mesh density plays a crucial role in getting an accurate solution. Meanwhile, the accuracy of the solution as well as computational cost is greatly dependent on the number of elements in the mesh. In this research work, mesh independence study is conducted at different refinement levels until a solution stability point is achieved. The details of different refinement levels are listed in Table 3. To examine the mesh independence study, maximum acoustic pressure and acoustic velocity are computed with different mesh refinement levels. Figure 5 describes the graphical representations of maximum acoustic pressure and velocity with varying different mesh refinement levels. The main goal of this mesh independence study is to ascertain the accuracy of simulation solution. A mesh refinement level of 5 is used for the current study having total number of elements and nodes are 30012 and 17821 respectively with average value of skewness 0.82. It can be observed clearly from Figure 6 that after refinement level of 5, there is no major difference in the results. Thus,

Preprints.org (www.preprints.org) | NOT PEER-REVIEWED | Posted: 27 April 2024 doi:10.20944/preprints202404.1780.v1

mesh refinement level of 5 is considered the best mesh which lies within acceptable range for current simulations considering the accuracy of the solution at appropriate computational cost.

Table 3. Description of mesh independence study.

Mesh Refinement Level	Number of Elements	Number of nodes	Acoustic Pressure (Pmax)	Acoustic Velocity (Vmax)
1	5616	3769	0.07314	0.000299
2	10080	6421	0.02564	0.000241
3	14592	9121	0.01944	0.000208
4	27332	16371	0.01761	0.000154
5	30012	17821	0.01685	0.000124
6	41856	24287	0.01626	0.000115
7	48062	27876	0.01605	0.000119

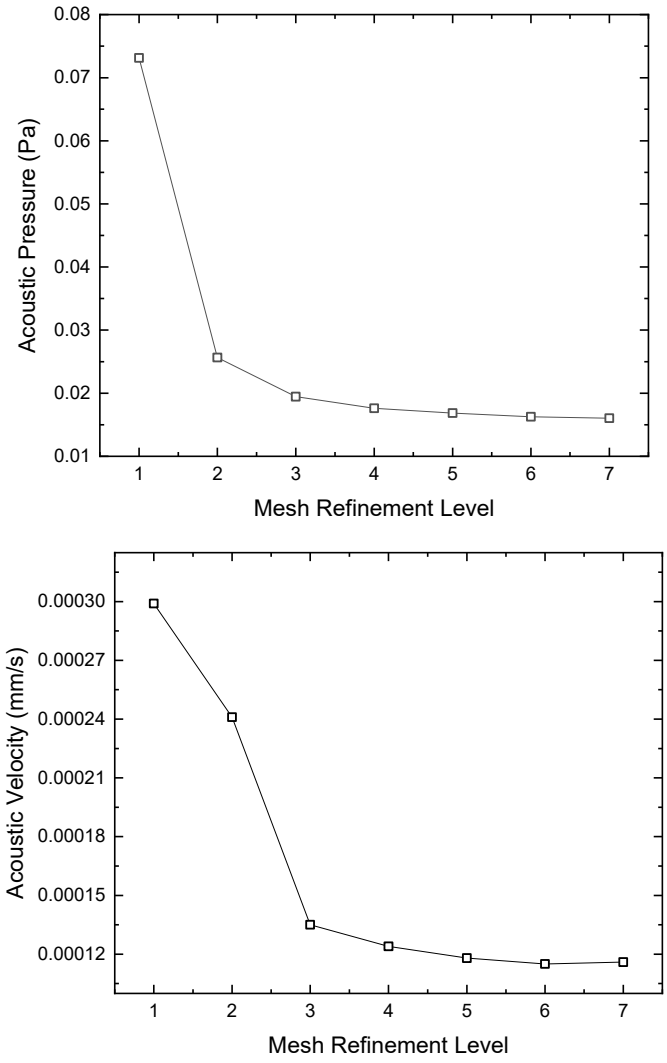

Figure 5. Variation of acoustic pressure and acoustic velocity with different mesh refinement levels.

Preprints.org (www.preprints.org) | NOT PEER-REVIEWED | Posted: 27 April 2024 doi:10.20944/preprints202404.1780.v1

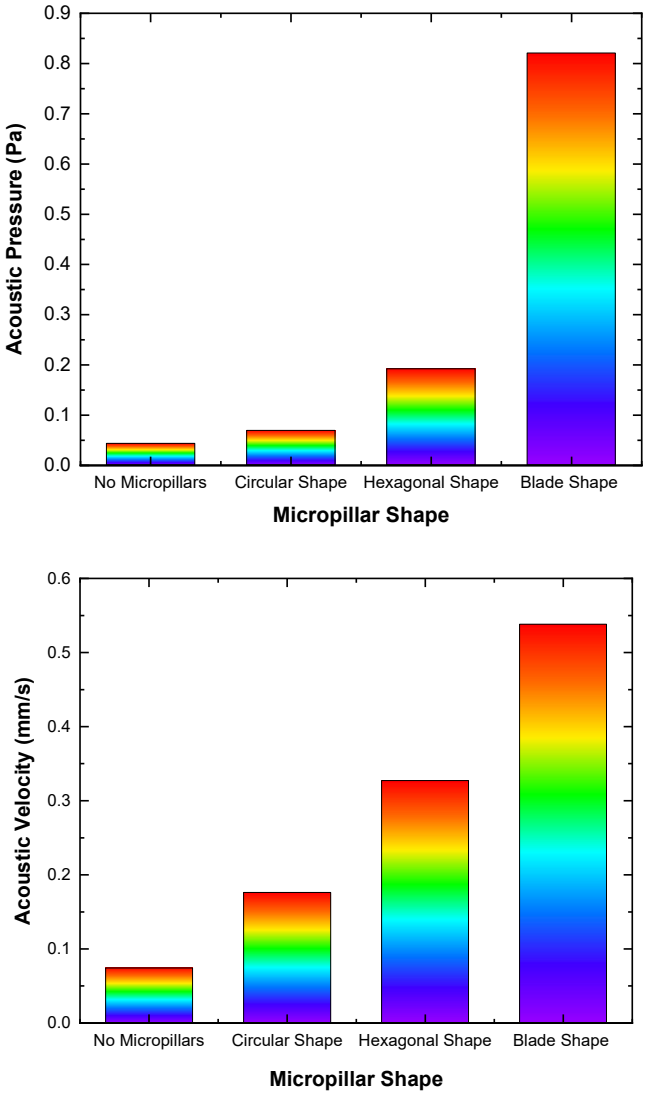

Figure 6. graphical representation of acoustic pressure and acoustic velocity with different micropillars shape.

4. Results and Discussion

This section describes the detail discussions about the numerical simulation outcomes such as characteristics of acoustic field, acoustic streaming and fluid mixing with different micropillar shapes and micropillar gaps and their impact on the mixing performance of hybrid microfluidics micro-mixer.

4.1. Acoustic Field

4.1.1. Effect of Micropillar Shapes

In this section, the characteristics of acoustic fields such as acoustic pressure and acoustic velocity are discussed for different micropillar shapes. Figure 6 represents the variation of acoustic pressure and acoustic velocity for different micropillars shapes. It can be observed from the graphical representations that the presence of micropillars in the microchamber results in a significant rise of acoustic pressure and acoustic velocity. The maximum value of acoustic pressure and acoustic velocity can be observed for the presence of blade shape micropillars as compared to other shapes. Similarly, the lowest value can be noted without micropillars. Based on these observations, it can be examined that micropillars increase the strength of acoustic field results in enhancing the mixing

Preprints.org (www.preprints.org) | NOT PEER-REVIEWED | Posted: 27 April 2024 doi:10.20944/preprints202404.1780.v1

performance of the micro-mixer. Moreover, contours of acoustic pressure and acoustic velocity are shown in Figure 7 and 8. It can be examined from Figure 7 that the acoustic excitation is more localized near the wall in the absence of micropillars while the addition of micropillars, the acoustic field provides more surface area to hit on which intense the field strength near the micropillars wall. Similarly, velocity field was also shown in Figure 8.

It is evident from figure 8 that the presence of micropillars generates more streaming velocity near the micropillars wall resulting in small vertexes which is helpful to enhance the mixing performance. Higher streaming can be seen for microchamber with blade shape micropillars. The maximum value of acoustic field such as acoustic pressure and acoustic velocity are observed for blade shape micropillars as compared to other micropillars shapes. Based on these observations, it can be examined that the inclusion of micropillars especially blade shape in the microchamber can be significantly consider to intense the mixing of two different heterogenous fluids.

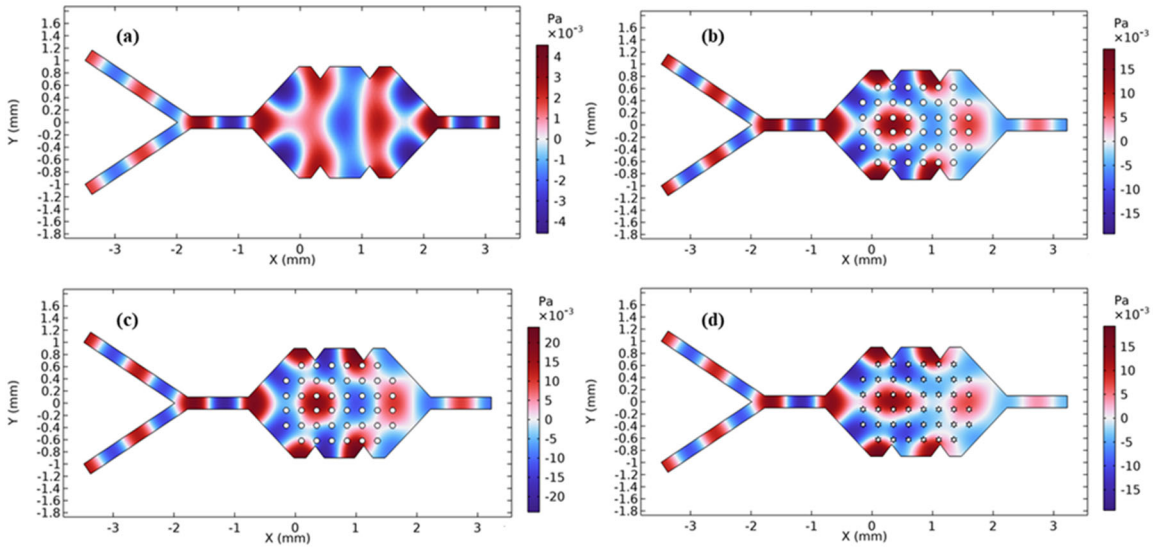

Figure 7. Acoustic pressure for different micropillars shapes; (a) No micropillars (b) Circular shape micropillars (c) hexagonal shape micropillars (d) blade shape micropillars.

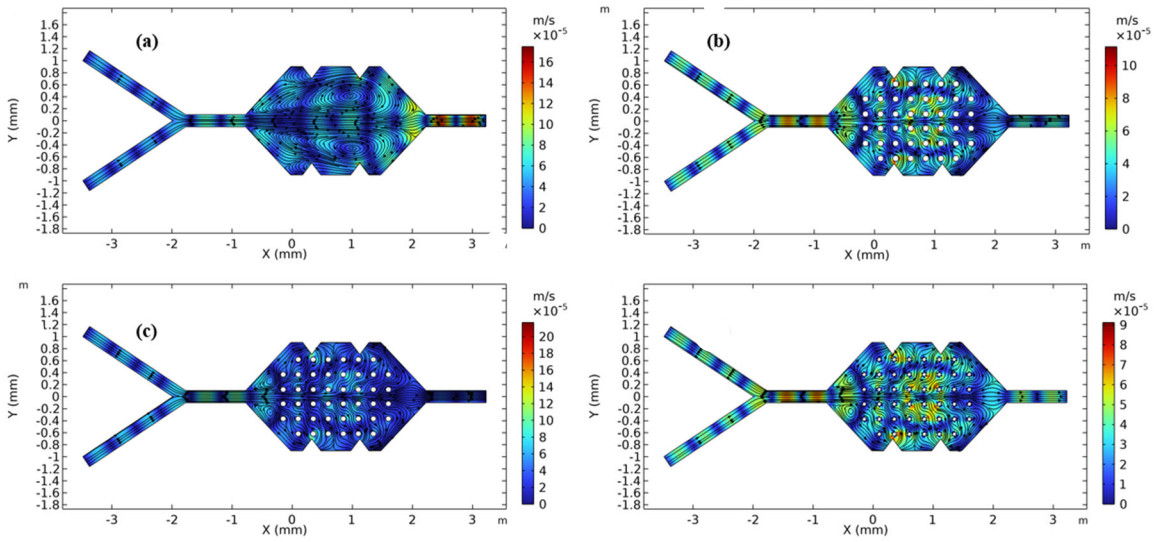

Figure 8. Acoustic velocity for different micropillars shapes; (a) No micropillars (b) Circular shape micropillars (c) hexagonal shape micropillars (d) b e shape micropillars.

Preprints.org (www.preprints.org) | NOT PEER-REVIEWED | Posted: 27 April 2024 doi:10.20944/preprints202404.1780.v1

4.1.2. Effect of Micropillars Gaps

This section describes the effect of micropillars gaps on acoustic field such as acoustic pressure and acoustic velocity. Figure 9 describes the graphical representations of acoustic pressure and acoustic velocity with different micropillars gaps. It can be observed from graphical representations that acoustic pressure and acoustic velocity increased with the decreasing of micropillar gaps. In addition, the blade shape micropillar has larger values of acoustic pressure and acoustic velocity as compared to other designs. Moreover, the maximum and minimum values of acoustic pressure and acoustic velocity are noted at micropillars gaps 0.15 mm and 0.25 mm respectively.

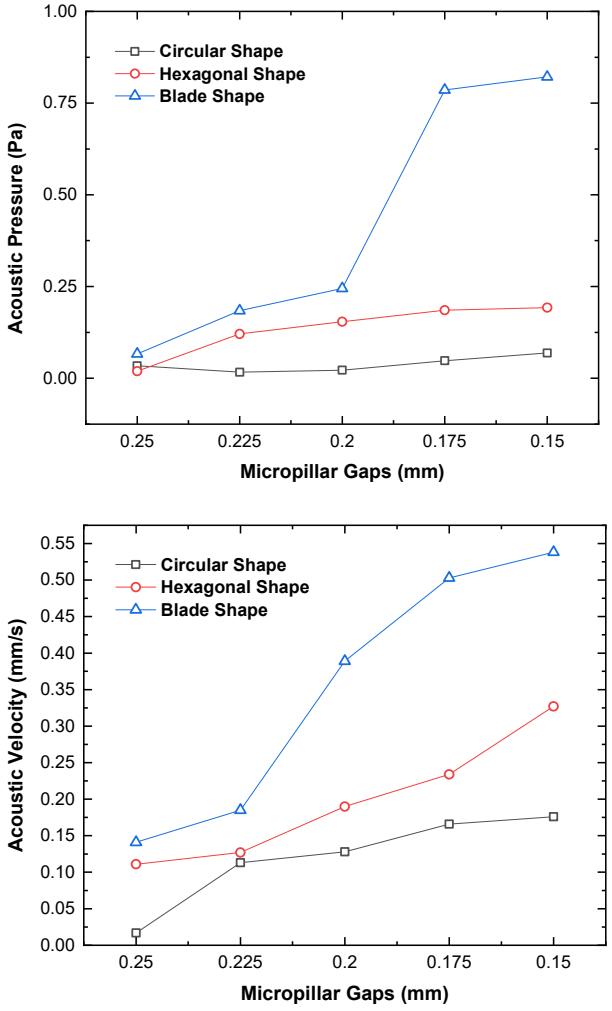

Figure 9. Variation of acoustic pressure and acoustic velocity with different micropillar gaps.

The main reason behind this increment of acoustic pressure and acoustic velocity with decreasing gaps is due to the higher surface area and more boundaries to hit on. Thus, more dense micropillars intense the field strength resulting in enhancement of mixing performance. It was also noted that compared to the other micropillars, the blade shape micropillars with 0.150 mm gap generate stronger acoustic field and according to computed results, the magnitude of acoustic pressure and acoustic velocity is approximately thrice and fourth times that of the case with no micropillars respectively. The acoustic pressure and acoustic velocity distribution with different micropillars gaps are also shown in Figures 10 and 11.

Preprints.org (www.preprints.org) | NOT PEER-REVIEWED | Posted: 27 April 2024 doi:10.20944/preprints202404.1780.v1

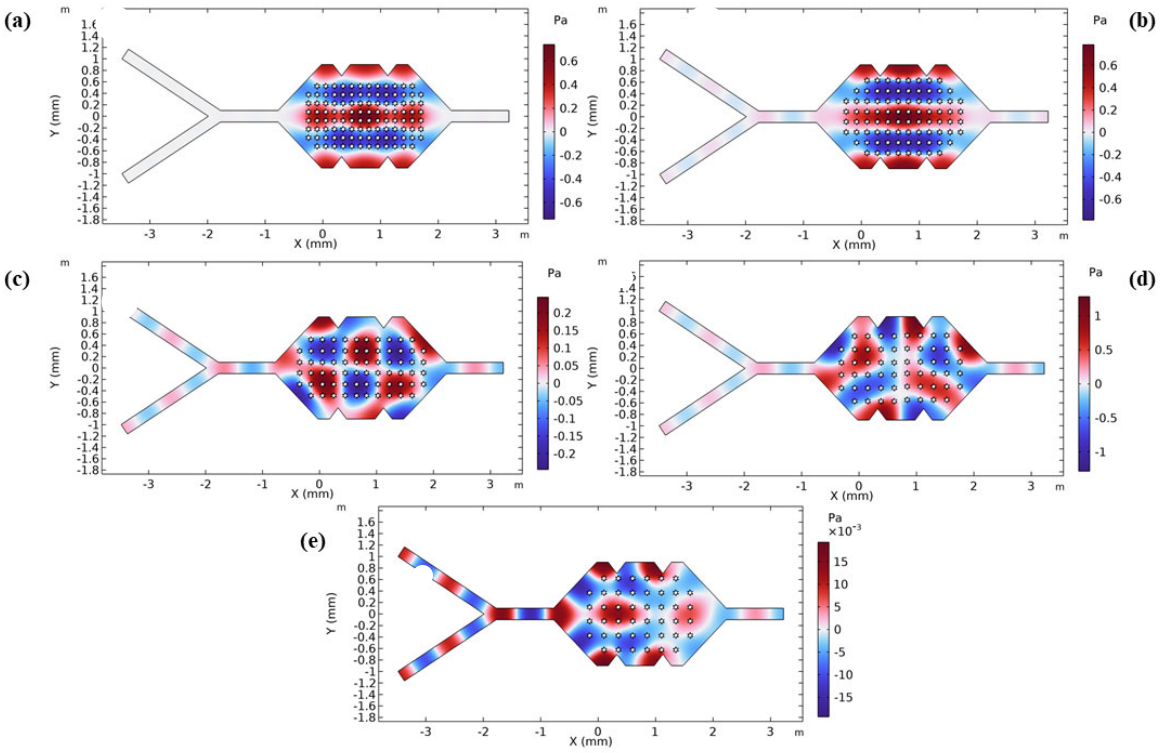

Figure 10. Distribution of acoustic pressure with different micropillar gaps; (a) 0.150 mm (b) 0.175 mm (c) 0.200 mm (d) 0.225 mm (e) 0.25 mm.

A stronger acoustic pressure field can be observed with 0.150 mm micropillar gap compared to others. Similarly, less acoustic pressure filed can be observed in case of with 0.250 mm micropillar gap. The reason behind this higher field strength is because of larger surface area and more boundaries to hit on results in increasing the diffusion of fluids as well as mixing performance. In the same way, distribution of acoustic velocity can also be noted in Figure 11. Higher small vertexes and acoustic velocity field generated in case of 0.150 mm micropillar gap compared to other cases. It can also be noted that less acoustic field is generated near the wall in case of 0.150 mm gap compared to the other cases. The reason behind this strong acoustic field near the micropillars is due to larger surface area and more boundaries in the microchamber as compared to the other cases.

Preprints.org (www.preprints.org) | NOT PEER-REVIEWED | Posted: 27 April 2024 doi:10.20944/preprints202404.1780.v1

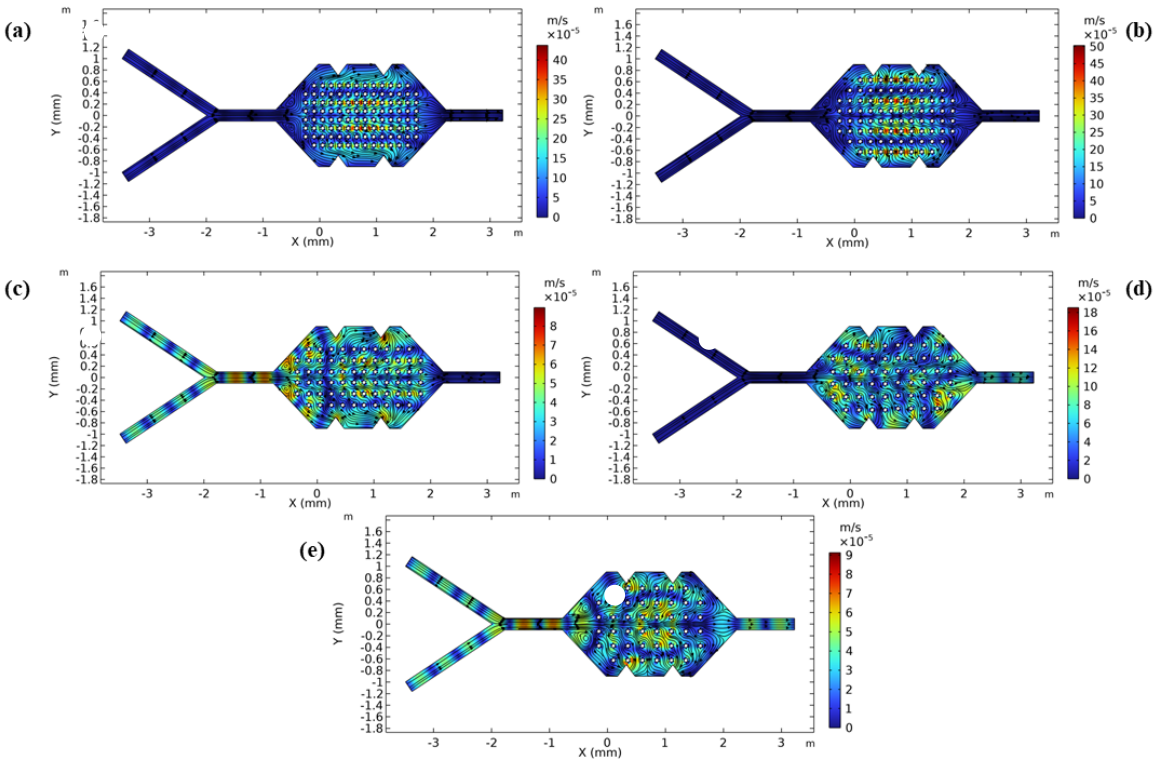

Figure 11. Distribution of acoustic velocity with different micropillar gaps; (a) 0.150 mm (b) 0.175 mm (c) 0.200 mm (d) 0.225 mm (e) 0.25 mm.

4.2. Fluid Mixing

In this section, the fluid mixing phenomena with different micropillar shapes and micropillar gaps and their effect on mixing performance are discussed. Although the physics behind the mixing of two different heterogenous fluids is entirely complicated, the degree of mixing can be quantified by measuring the degree of folding and stretching of fluids as well as simultaneous diffusion of species [41]. The process of stretching and folding in the case of two different heterogenous fluids is followed by the crumbling of stretched layers into smaller components, along with the simultaneous diffusion of species [42]. One of the key goals of this study is to intensify the mixing of two different heterogenous fluids. The hybrid approach is one of best ways to attain homogeneous mixing of two different heterogenous fluids by employing the acoustic streaming as an active approach and micropillars as a passive approach. The interfacial region near the micropillar wall is then significantly stretched and folded by intense micro vortices creating lamellar structures. The mass diffusion rate of two different heterogenous fluids intensifies due to larger contact area in the presence of micropillars.

4.2.1. Effect of Micropillar Shapes

The quality of mixing can be quantified by determining the mixing index which is given by Equations (1, 2 & 3). Figure 12 shows the graphical representation of variation of mixing index for different micropillar shapes. Because of hybrid approach and inclusion of micropillars, higher mixing index can be observed compared to no micropillars. In addition, among all shapes, blade shape micropillars get higher mixing index than other shapes. The reason behind this higher mixing index is due to providing more contact area and boundaries in case of with blade shape micropillars compared to other cases. The concentration distribution of two different species can be seen in Figure 13. It can be clearly observed that maximum and minimum diffusion of species concentration is in case of with blade shape micropillars and with no micropillars case respectively.

The magnitude of mixing index for the case of blade shape micropillars and with no micropillars are 0.95 and 0.72 respectively. Because of laminar flow nature in microfluidics systems, mixing occurs

Preprints.org (www.preprints.org) | NOT PEER-REVIEWED | Posted: 27 April 2024 doi:10.20944/preprints202404.1780.v1

due to diffusion of molecules. Thus, the inclusion of micropillars provides more contact area generate more small vertexes resulting in enhancing the mixing performance. Based on the observations and computed findings, the presence of micropillars in the microfluidics chamber intense the mixing performance.

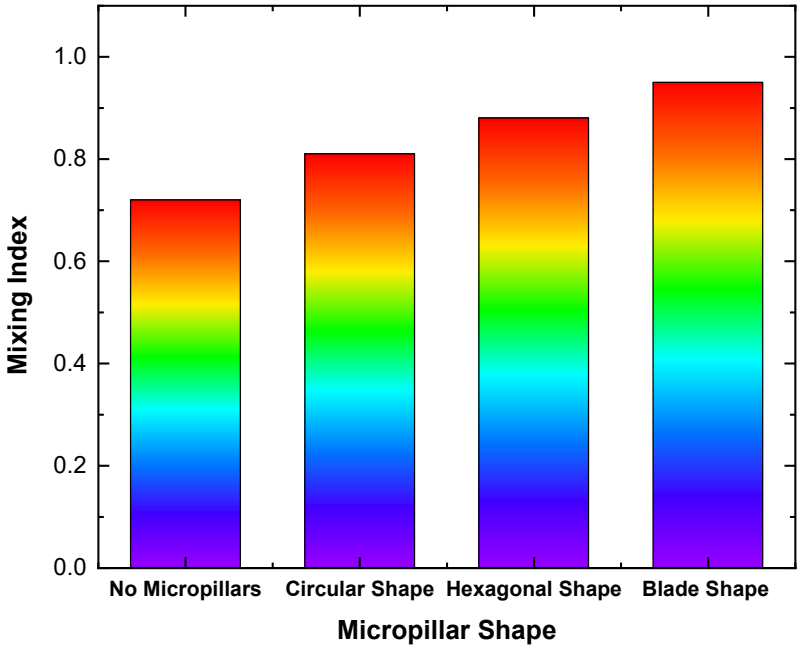

Figure 12. Variation of mixing index for different micropillar shapes.

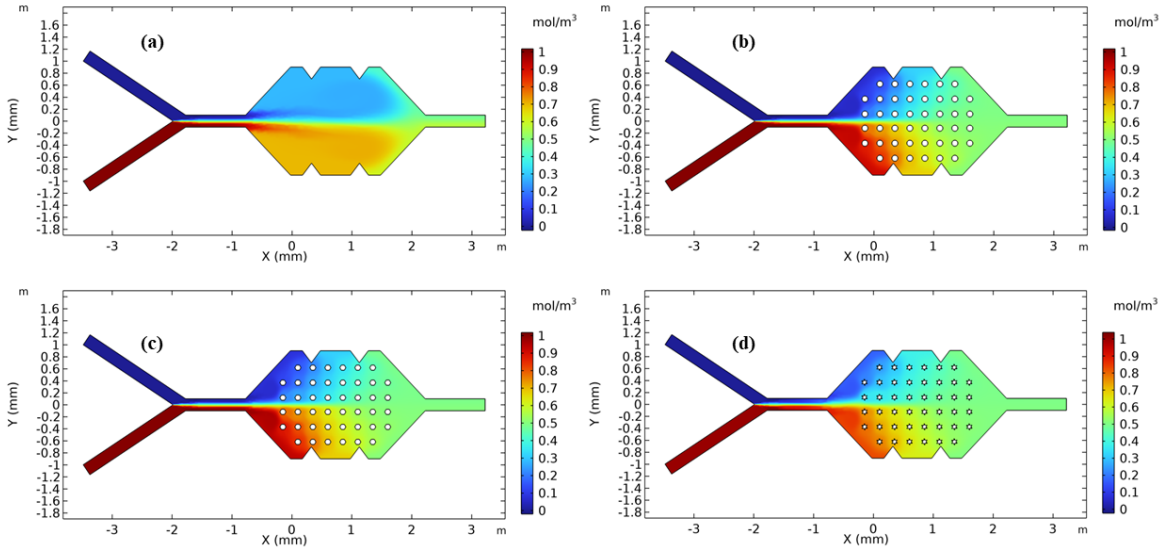

Figure 13. Distribution of species concentrations; (a) No micropillar (b) Circular shape micropillar (c) hexagonal shape micropillars (d) Blade shape micropillars.

4.2.2. Effect of Micropillar Gaps

In this section, the effect of micropillar gaps on mixing performance of microfluidic micro-mixer is investigated. Figure 14 represents the graphical representation of variation of mixing index by varying the micropillar gaps. It is evident that mixing index increased linearly by decreasing the micropillar gaps. The higher mixing index can be observed for 0.150 mm gap while lower mixing index can be observed for 0.250 mm gap. The reason behind this larger value is due to the larger contact area and more boundaries to hit on in case of smaller micropillar gaps. On the other hand,

Preprints.org (www.preprints.org) | NOT PEER-REVIEWED | Posted: 27 April 2024 doi:10.20944/preprints202404.1780.v1

among all micropillar shapes, the higher value of mixing index can be noted in case of blade shape micropillars. The reason behind this larger value in such case is due to larger contact area and intense micro-vortices near the micropillar walls compared to other shapes. Moreover, distribution of concentrations of species with different micropillar gaps are also shown in Figure 15. The lower diffusion of species transports as well as mixing can be clearly observed in case of 0.250 mm micropillar gap. Similarly, higher mixing and diffusion rate can be observed in the case of 0.150 mm micropillar gap. The main reason behind this larger mixing index with small micropillar gaps is due to the larger contact area results in generating more micro-vortices.

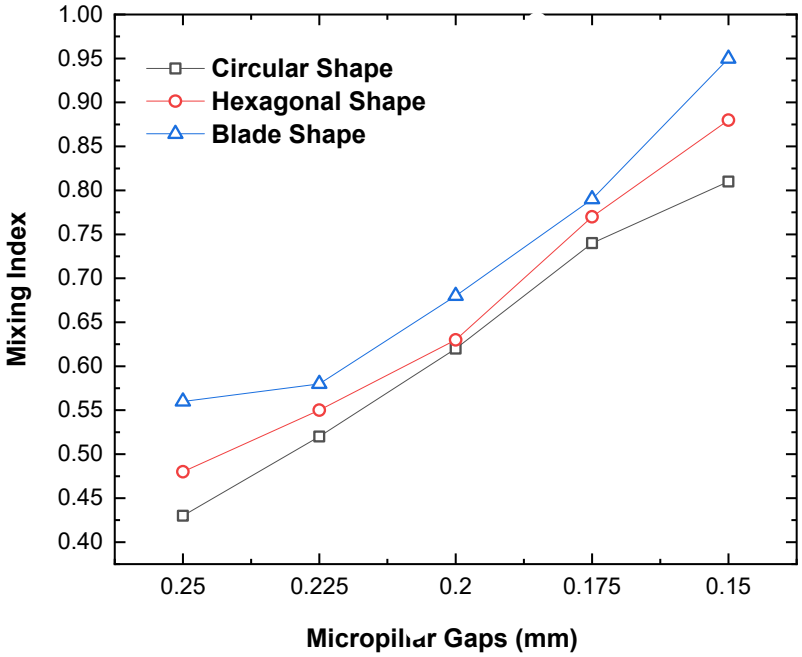

Figure 14. Variation of mixing index with different micropillar gaps.

In comparative examination of the performance of different micropillar shapes and micropillar gaps, it was investigated that the presence of micropillars in the microchamber of the microfluidics system is significant in improving the mixing performance of two different heterogeneous fluids. In addition, blade shape micropillars with 0.150 mm gap deliver best outcomes and perform better as compared to other cases. As discussed earlier, this is due to employing hybrid actuation approach and higher diffusion rate of species concentrations. Finally. It is concluded that the proposed hybrid microfluidic micro-mixer can be used for high quality mixing and reaction kinetics.

Preprints.org (www.preprints.org) | NOT PEER-REVIEWED | Posted: 27 April 2024 doi:10.20944/preprints202404.1780.v1

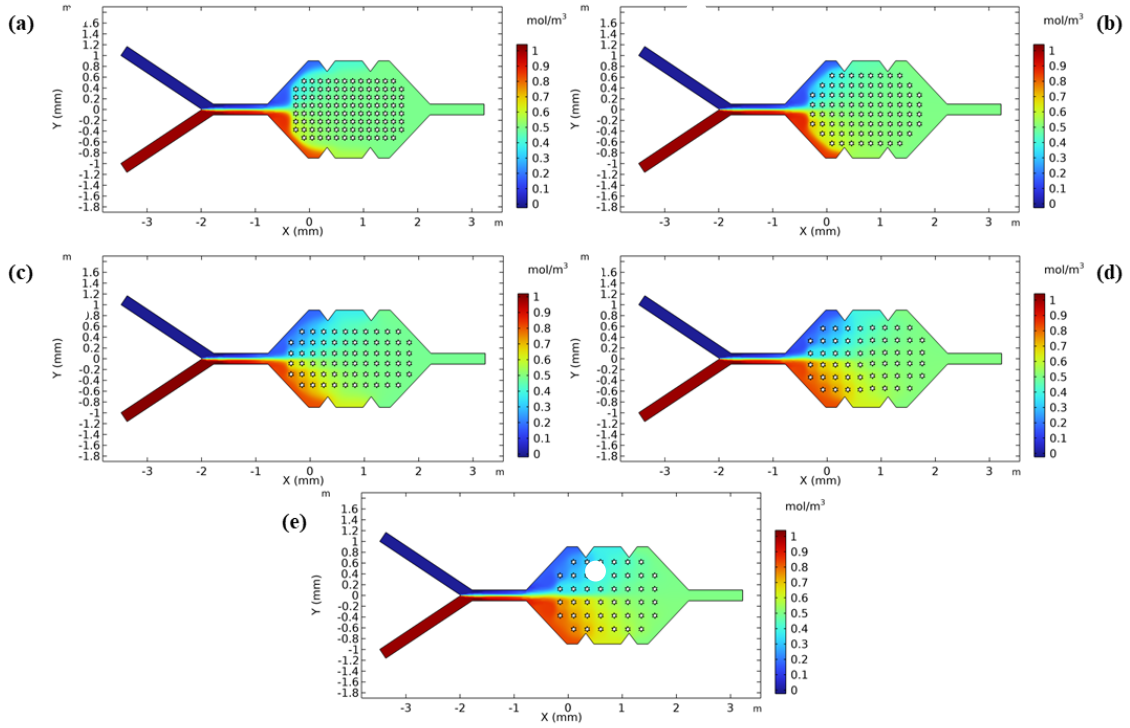

Figure 15. Distribution of species concentration with different micropillar gaps.

5. Conclusions

This paper investigated the performance of microfluidics micro-mixer using hybrid actuation approach such as active (Acoustic) and passive (inclusion of micropillars in the microfluidics chamber). The simulations were performed for four different micro-mixer designs such as with circular shape micropillars, hexagonal shape micropillars, blade shape micropillars and without micropillars. In addition, different micropillars gaps such as 0.150 mm, 0.175 mm, 200 mm, 225 mm, and 250 mm were also used to investigate the mixing performance. The detailed conclusions drawn from this study are described below.

1. The performance of microfluidics micro-mixer is greatly affected by the inclusion of micropillars compared to the case with no micropillars. The presence of micropillars in the microfluidics chamber increases the micro vortices as well as strengthens the acoustic field.
2. Similarly, shapes of micropillars are also impacted on flow characteristics as well as mixing performance of microfluidics micro-mixer. Various micropillars shapes such as circular, hexagonal and blade were investigated and compared to the case with no micropillars. The inclusion of blade shape micropillars delivers the best outcomes compared to other shapes.
3. The performance of microfluidics micro-mixer was also investigated with different micropillars gaps and found that the mixing performance increased with the decreasing of micropillars gaps. The reason behind this increment in performance is due to larger surface areas and more boundaries to generate higher micro vortices as well as strengthening the acoustic field near the micropillars walls. The maximum performance achieved with micropillar gap of 0.150 mm.
4. The maximum and minimum magnitude values of 0.95 and 0.72 of mixing index are achieved respectively with the inclusion of blade shape micropillars and 0.150 mm micropillar gap.
5. Based on the current research work, further work is required for the optimization of hybrid microfluidics micro-mixer based on various micropillars arrangements. In addition, acoustic structure analysis with different materials and geometrical parameters is also required to examine the structural stability and structural strength of micropillars.

Author Contributions: Conceptualization, M.W. and G.J.; methodology, M.W. and A.P.; software, M.W. and G.J.; validation, A.P., V.N. and G.J.; formal analysis, V.N. and A.P.; investigation, M.W., A.P. and G.J.; writing—

Preprints.org (www.preprints.org) | NOT PEER-REVIEWED | Posted: 27 April 2024 doi:10.20944/preprints202404.1780.v1

original draft preparation, M.W.; writing—review and editing, A.P. and G.J. All authors have read and agreed to the published version of the manuscript.

Funding: This research received no external funding.

References

1. M. Juraeva and D. J. Kang, "Mixing performance of a cross-channel split-and-recombine micro-mixer combined with mixing cell," *Micromachines*, vol. 11, no. 7, 2020, doi: 10.3390/mi11070685.
2. T. Wan, B. Wang, Q. Han, J. Chen, B. Li, and S. Wei, "A review of superhydrophobic shape-memory polymers: Preparation, activation, and applications," *Appl. Mater. Today*, vol. 29, no. July, p. 101665, 2022, doi: 10.1016/j.apmt.2022.101665.
3. S. Prakash and S. Kumar, "Fabrication of microchannels: A review," *Proc. Inst. Mech. Eng. Part B J. Eng. Manuf.*, vol. 229, no. 8, pp. 1273–1288, 2015, doi: 10.1177/0954405414535581.
4. D. Bahrami, A. A. Nadooshan, and M. Bayareh, "Effect of non-uniform magnetic field on mixing index of a sinusoidal micromixer," *Korean J. Chem. Eng.*, vol. 39, no. 2, pp. 316–327, 2022, doi: 10.1007/s11814-021-0932-z.
5. B. Lee *et al.*, "Characterization of passive microfluidic mixer with a three-dimensional zig-zag channel for cryo-EM sampling," *Chem. Eng. Sci.*, vol. 281, no. May, p. 119161, 2023, doi: 10.1016/j.ces.2023.119161.
6. E. Tripathi, P. K. Patowari, and S. Pati, "Numerical investigation of mixing performance in spiral micromixers based on Dean flows and chaotic advection," *Chem. Eng. Process. - Process Intensif.*, vol. 169, no. July, p. 108609, 2021, doi: 10.1016/j.cep.2021.108609.
7. C. Bai, W. Zhou, S. Yu, T. Zheng, and C. Wang, "A surface acoustic wave-assisted micromixer with active temperature control," *Sensors Actuators A Phys.*, vol. 346, no. August, p. 113833, 2022, doi: 10.1016/j.sna.2022.113833.
8. C. Kumar *et al.*, "Modeling of mass transfer enhancement in a magnetofluidic micromixer," *Phys. Fluids*, vol. 31, no. 6, 2019, doi: 10.1063/1.5093498.
9. M. Rahimi, B. Aghel, B. Hatamifar, M. Akbari, and A. A. Alsairafi, "CFD modeling of mixing intensification assisted with ultrasound wave in a T-type microreactor," *Chem. Eng. Process. Process Intensif.*, vol. 86, pp. 36–46, 2014, doi: 10.1016/j.cep.2014.10.006.
10. H. Jalili, M. Raad, and D. A. Fallah, "Numerical study on the mixing quality of an electroosmotic micromixer under periodic potential," *Proc. Inst. Mech. Eng. Part C J. Mech. Eng. Sci.*, vol. 234, no. 11, pp. 2113–2125, 2020, doi: 10.1177/0954406220904089.
11. Y. Gong and X. Cheng, "Numerical investigation of electroosmotic mixing in a contraction–expansion microchannel," *Chem. Eng. Process. - Process Intensif.*, vol. 192, no. February, p. 109492, 2023, doi: 10.1016/j.cep.2023.109492.
12. S. Xiong, X. Chen, H. Chen, Y. Chen, and W. Zhang, "Numerical study on an electroosmotic micromixer with rhombic structure," *J. Dispers. Sci. Technol.*, vol. 42, no. 9, pp. 1331–1337, 2021, doi: 10.1080/01932691.2020.1748644.
13. B. Mondal, S. K. Mehta, S. Pati, and P. K. Patowari, "Numerical analysis of electroosmotic mixing in a heterogeneous charged micromixer with obstacles," *Chem. Eng. Process. - Process Intensif.*, vol. 168, no. July, p. 108585, 2021, doi: 10.1016/j.cep.2021.108585.
14. K. N. Vasista, S. K. Mehta, and S. Pati, "Electroosmotic mixing in a microchannel with heterogeneous slip dependent zeta potential," *Chem. Eng. Process. - Process Intensif.*, vol. 176, no. April, p. 108940, 2022, doi: 10.1016/j.cep.2022.108940.
15. L. Tata Rao, S. Goel, S. Kumar Dubey, and A. Javed, "Performance Investigation of T-Shaped Micromixer with Different Obstacles," *J. Phys. Conf. Ser.*, vol. 1276, no. 1, 2019, doi: 10.1088/1742-6596/1276/1/012003.
16. A. Farahinia and W. J. Zhang, "Numerical investigation into the mixing performance of micro T-mixers with different patterns of obstacles," *J. Brazilian Soc. Mech. Sci. Eng.*, vol. 41, no. 11, 2019, doi: 10.1007/s40430-019-2015-1.
17. A. Xia *et al.*, "Numerical and Experimental Investigation on a 'Tai Chi'-Shaped Planar Passive Micromixer," *Micromachines*, vol. 14, no. 7, 2023, doi: 10.3390/mi14071414.
18. Y. Jiang and Y. Zhang, "High performance micromixers by 3D printing based on split-and-recombine modules and twisted-architecture microchannel," *Proc. 5th Int. Conf. Intell. Hum. Syst. Integr. (IHSI 2022) Integr. People Intell. Syst. Febr. 22–24, 2022, Venice, Italy*, vol. 22, no. Ihsi 2022, 2022, doi: 10.54941/ahfe1001085.
19. Z. Wang, X. Yan, Q. Zhou, Q. Wang, D. Zhao, and H. Wu, "A Directly Moldable, Highly Compact, and Easy-for-Integration 3D Micromixer with Extraordinary Mixing Performance," *Anal. Chem.*, vol. 95, no. 23, pp. 8850–8858, 2023, doi: 10.1021/acs.analchem.3c00335.
20. Y. Shao *et al.*, "Cross-channel microfluidic device for dynamic control of concentration and velocity by the electroosmotic drive," *Chem. Eng. Sci.*, vol. 281, no. July, p. 119139, 2023, doi: 10.1016/j.ces.2023.119139.
21. K. Ward and Z. H. Fan, "Mixing in microfluidic devices and enhancement methods," *J. Micromechanics Microengineering*, vol. 25, no. 9, 2015, doi: 10.1088/0960-1317/25/9/094001.

Preprints.org (www.preprints.org) | NOT PEER-REVIEWED | Posted: 27 April 2024 doi:10.20944/preprints202404.1780.v1

22. J. B. You *et al.*, "PDMS-based turbulent microfluidic mixer," *Lab Chip*, vol. 15, no. 7, pp. 1727–1735, 2015, doi: 10.1039/c5lc00070j.
23. X. Chen and H. Lv, "New insights into the micromixer with Cantor fractal obstacles through genetic algorithm," *Sci. Rep.*, vol. 12, no. 1, pp. 1–17, 2022, doi: 10.1038/s41598-022-08144-w.
24. M. Xiong, J. Yang, X. Ding, H. Li, and H. Zhang, "Topology optimization design of micromixer based on principle of Tesla valve: An experimental and numerical study," *Chem. Eng. Process. - Process Intensif.*, vol. 193, no. August, p. 109560, 2023, doi: 10.1016/j.cep.2023.109560.
25. Z. Chen, Z. Pei, X. Zhao, J. Zhang, J. Wei, and N. Hao, "Acoustic microreactors for chemical engineering," *Chem. Eng. J.*, vol. 433, no. P2, p. 133258, 2022, doi: 10.1016/j.cej.2021.133258.
26. H. Ahmed, J. Park, G. Destgeer, M. Afzal, and H. J. Sung, "Surface acoustic wave-based micromixing enhancement using a single interdigital transducer," *Appl. Phys. Lett.*, vol. 114, no. 4, 2019, doi: 10.1063/1.5079815.
27. H. Lim, S. M. Back, H. Choi, and J. Nam, "Acoustic mixing in a dome-shaped chamber-based SAW (DC-SAW) device," *Lab Chip*, vol. 20, no. 1, pp. 120–125, 2020, doi: 10.1039/c9lc00820a.
28. X. Li, J. Huffman, N. Ranganathan, Z. He, and P. Li, "Acoustofluidic enzyme-linked immunosorbent assay (ELISA) platform enabled by coupled acoustic streaming," *Anal. Chim. Acta*, vol. 1079, pp. 129–138, 2019, doi: 10.1016/j.aca.2019.05.073.
29. "Microfluidic Mixing," *SpringerReference*, no. 2, pp. 1–13, 2011, doi: 10.1007/springerreference_67173.
30. G. Gharib *et al.*, "Biomedical Applications of Microfluidic Devices: A Review," *Biosensors*, vol. 12, no. 11, 2022, doi: 10.3390/bios12111023.
31. A. Francesko, V. F. Cardoso, and S. Lanceros-Méndez, *Lab-on-a-chip technology and microfluidics*. 2019. doi: 10.1016/B978-0-12-812659-2.00001-6.
32. M. A. Khan, M. Suhaib, and M. A. Ansari, "Investigations on fluid flow and mixing in fractal tree like biomimetic microchannel based on Murray's law," *Chem. Eng. Process. - Process Intensif.*, vol. 194, no. October, p. 109564, 2023, doi: 10.1016/j.cep.2023.109564.
33. F. Liu *et al.*, "An inverted micro-mixer based on a magnetically-actuated cilium made of Fe doped PDMS," *Smart Mater. Struct.*, vol. 25, no. 9, 2016, doi: 10.1088/0964-1726/25/9/095049.
34. W. Kim, B. Cha, J. S. Jeon, and J. Park, "Acoustofluidic control of chemical concentration within picoliter droplets in a disposable microfluidic chip," *Sensors Actuators B Chem.*, vol. 393, no. January, p. 134132, 2023, doi: 10.1016/j.snb.2023.134132.
35. E. Jalilvand, A. Shamloo, and M. H. Gangaraj, "Computational study of an integrated microfluidic device for active separation of RBCs and cell lysis," *Chem. Eng. Process. - Process Intensif.*, vol. 174, no. March, p. 108891, 2022, doi: 10.1016/j.cep.2022.108891.
36. R. E. Pawinanto, J. Yunas, and A. M. Hashim, "Design optimization of active microfluidic mixer incorporating micropillar on flexible membrane," *Microsyst. Technol.*, vol. 25, no. 4, pp. 1203–1209, 2019, doi: 10.1007/s00542-018-4134-5.
37. H. Bruus, "Acoustofluidics 1: Governing equations in microfluidics," *Lab Chip*, vol. 11, no. 22, pp. 3742–3751, 2011, doi: 10.1039/c1lc20658c.
38. H. Bruus, *Theoretical Microfluidics*, no. January 2008. 1997. doi: 10.1093/oso/9780199235087.001.0001.
39. H. Bruus, "Governing Equations in Micro ◎ uidics," pp. 1–28.
40. "Chapter 18. Theory," vol. 0, pp. 1–52, 2002, [Online]. Available: http://www.ce.utexas.edu/prof/Novoselac/classes/ARE372/handouts/CFD_theory.pdf
41. J.M. Ottino, The Kinematics of Mixing : Stretching, Chaos and Transport, in: Cambridge Texts in Applied Mathematics, Cambridge University Press, 2004. [Online]. Available: https://books.google.lt/books?id=8OLVcbRoNSgC&lpg=PP1&hl=lt&pg=PP1#v=onepage&q&f=false
42. C. Barman and A. Bandopadhyay, "Mixing intensification in an acoustofluidic micromixer aided with micro-pillars," *Chem. Eng. Process. - Process Intensif.*, vol. 194, no. November, p. 109604, 2023, doi: 10.1016/j.cep.2023.109604.

Disclaimer/Publisher's Note: The statements, opinions and data contained in all publications are solely those of the individual author(s) and contributor(s) and not of MDPI and/or the editor(s). MDPI and/or the editor(s) disclaim responsibility for any injury to people or property resulting from any ideas, methods, instructions or products referred to in the content.